Journal of Alloys and Compounds 687 (2016) 312–319

Contents lists available at ScienceDirect

Journal of Alloys and Compounds

journal homepage: http://www.elsevier.com/locate/jalcom

Effect of La addition on the particle characteristics, mechanical and electrical properties of in situ Cu-TiB_2 composites

Cunlei Zou, Huijun Kang, Wei Wang, Zongning Chen, Rengeng Li, Xiaoxia Gao, Tingju Li, Tongmin Wang*

Key Laboratory of Solidification Control and Digital Preparation Technology (Liaoning Province), School of Material Science and Engineering, Dalian University of Technology, Dalian, 116024, China

ARTICLE INFO

Article history:
Received 18 April 2016
Received in revised form
12 June 2016
Accepted 14 June 2016
Available online 16 June 2016

Keywords:
In situ Cu-TiB_2 composite
Rare earth
Particle distribution
Mechanical properties
Electrical conductivity

ABSTRACT

In situ Cu-TiB_2 composites can be synthesized via metallurgical process by mixing Cu-B and Cu-Ti master alloys before casting. In this paper, La, as a rare earth element was added to the composites to improve the comprehensive properties and the effects of its addition on the microstructures, mechanical and electrical characteristics of Cu-TiB_2 composites were investigated. Results show that addition of La significantly diminishes the average size and facilitates a homogeneous distribution of TiB_2 particles in the copper matrix. As a result, an improvement in mechanical properties was achieved. In particular, a remarkable change in the conductivity of the composites appears with the variation of La content. The mechanisms of particle refinement and improvements in properties by La alloying were analyzed.

1. Introduction

High strength and high conductivity copper alloys have many industrial applications, such as rail transit contact wires, integrated circuit lead frames, the electrodes of resistance welding and so on [1–4]. Owing to desired combination of mechanical properties, electrical conductivity and thermal conductivity, copper matrix composites (CMCs) has attracted so much attention in recent years. Many routes, such as powder metallurgy, mechanical alloying, internal oxidation, self-propagating high-temperature synthesis (SHS), etc. have been developed to fabricate CMCs [5–11]. Compared to the conventional ex situ methods, in situ reaction synthesis produces superior wetting interface between particle and matrix, and the CMCs thus prepared exhibit preferable integrated performances (i.e. tensile strength and electrical conductivity). Therefore, in situ reaction synthesis, as a promising route to fabricate high quality CCMs, has been extensively investigated in the past fifteen years [12–15]. Among various in situ routes, the casting process is of particular interest owing to its lower cost and potential for mass production.

Compared to the unreinforced copper, the improved properties of the CMCs mainly originate from the second-phase particles, such as carbides (TiC, SiC), borides (TiB_2, ZrB_2) and oxides (Al_2O_3) [10,16–21]. Among these particles, TiB_2 is deemed to be a good candidate to reinforce CMCs because of its high hardness value (HV: 34 GPa), high elastic modulus (574 GPa), good electrical conductivity (14.4 μΩ cm) and good thermodynamic stability [22]. Moreover, TiB_2 particles are thermodynamically stable and can easily form through in situ reactions between titanium and boron elements in copper melt [23,24]. In this process, in order to maximize the reinforcing efficiency of TiB_2, it is desirable to have the tiny in situ TiB_2 particles as much as possible homogeneously distributed throughout the copper matrix according to the Orowan strengthening mechanism. This goal, however, is generally hard to meet since the high surface energy of TiB_2 particles will lead to severe agglomeration of TiB_2 particles after solidification. It has been reported in the literature that rare earth elements are widely used in various processes to improve the microstructures and mechanical properties of copper and CMCs [25–29]. These beneficial effects were attributed to the special physical and chemical characteristics of rare earth elements. For example, La could effectively refine the microstructures in the as-cast Cu-Zr composites, resulting in the improvement of the hardness and conductivity simultaneously [30]. Therefore, the rare earth elements seem to be good candidates

* Corresponding author.
E-mail address: tmwang@dlut.edu.cn (T. Wang).

http://dx.doi.org/10.1016/j.jallcom.2016.06.129
0925-8388/

to modify the properties of copper and CMCs for its less cost.

In this study, La, chosen as a representative of the rare earth elements, was added to prepare in situ TiB_2 particulate reinforced CMCs. The effects of La on the particle size and distribution of TiB_2, mechanical properties and conductivity of Cu-TiB_2 composites were examined.

2. Experimental procedure

Pure Cu (99.97% purity, weight percentage, all in the same unit unless otherwise specified) was used as the matrix. Cu-5B and Cu-10Ti master alloys were used as the reactive agents. Pure La (99.99% purity) was added into the composites. The composites were prepared in a vacuum medium frequency induction melting furnace. When the temperature of Cu melt reached 1300 °C, La, Cu-B and Cu-Ti master alloys were incorporated into the melt sequentially. After holding for 5 min, TiB_2 particles were formed via chemical reactions between Ti and B. Subsequently, the melt was poured into a cylindrical graphite mould (45 mm in diameter and 220 mm in height) which was preheated to 300 °C. After homogeneous annealing at 960 °C for 3 h, the as-cast billets were rolled at 850 °C with a 17% reduction (from 30 mm to 25 mm) and then further rolled to 1.5 mm with a total of 94% reduction at room temperature. A series of Cu-1 wt% TiB_2 composites with 0.02, 0.04, 0.06 and 0.08 wt% La were produced. For comparison, a reference sample without La addition was also prepared.

The samples were mechanically ground, polished and etched with a corrosive agent (3 g $FeCl_3$, 2 mL HCl and 95 mL C_2H_5OH) for metallographic examination. The microstructure and TiB_2 distribution in the copper matrix were observed under a scanning electron microscopy (SEM, Zeiss supra 55) operated at secondary electron mode with an accelerating voltage of 15 kV complemented by energy-dispersive spectroscopy (EDS). Phases in the in situ Cu-1TiB_2 composites with and without La were identified using an X-ray diffractometer (XRD, EMPYREAN, Cu Kα radiation, scanning from 20° to 100° in 2θ at a scanning speed of 0.26738°/s). The morphology of TiB_2 particles, interface between TiB_2 and copper matrix and the dislocations and twin crystals in samples were investigated using Talos F200x field emission transmission electron microscopy at an accelerating voltage of 200 kV. The tensile specimens, with a dimension of 35 mm gauge length, 5 mm diameter, were machined from the samples according to the ASTME8 standard test methods for tension testing of metallic materials. Tensile tests with cross head speed of 2 mm min^{-1} were conducted at room temperature. Vickers hardness tests were performed under a load of 100 g for 10 s using a Vickers hardness tester (MH-6L). For each test, five measurements were performed at an interval of 1 mm and average experimental data were recorded. The electrical conductivities were measured by D60K eddy current conductivity meter. The samples size was bigger than 15 mm diameter and thicker than 2 mm. And five measurements were also performed for each test.

3. Results and discussions

3.1. Microstructures investigations

3.1.1. XRD analysis

The XRD patterns of Cu-1TiB_2% and Cu-1TiB_2-0.04La were shown in Fig. 1. The XRD spectrum clearly demonstrated that TiB_2 was successfully synthesized in the copper matrix via the casting process. But comparing the two spectra one may see that addition of La did not noticeably change the phase composition of the composite due to its trace amount of 0.04 wt%.

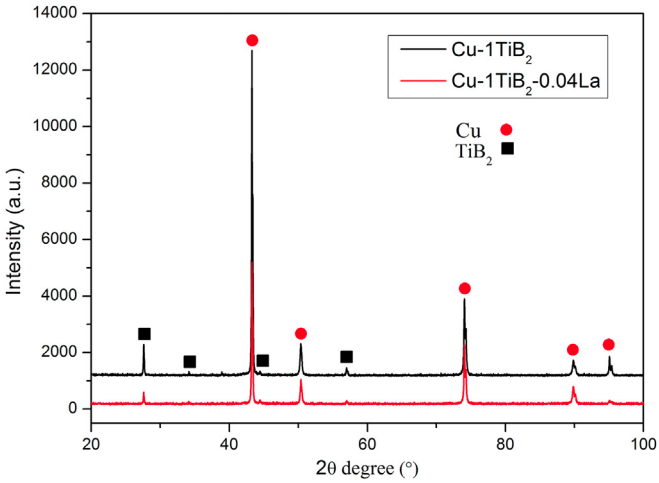

Fig. 1. XRD patterns of Cu-1 wt% TiB_2 and Cu-1 wt% TiB_2-0.04 wt% La composites.

3.1.2. SEM analysis

The microstructure of Cu-1TiB_2 with different mass faction of La are presented in Fig. 2. Fig. 2 (f) is the EDS analysis of the blocky particle in the Cu-TiB_2 sample with 0.04 La. From the SEM micrographs of the composites in Fig. 2a–c, a significant decreasing trend in particle size can be observed. The detailed size distribution of TiB_2 particles in the composites with different La content is plotted in Fig. 3. From the quantitative data, it is easy to see that the average particle size is refined from 1132 nm to 423 nm when the La addition is increased from none to 0.04 wt%, whilst an increasing trend followed once the La addition rate exceeded 0.04 wt%.

Besides, change in the morphology of the TiB_2 particles is also noticed in Fig. 2. An irregular angular shape was gradually smoothened and refined to round morphology, along with the decrease in particle size. The roundness has been defined to describe the morphology of particles. And it was calculated by the equation: Roundness $= 4\pi s/l^2$ [31], where l is the perimeter and s is the area of the particles in the SEM image which were measured by image-pro plus. According to the equation, the roundness of TiB_2 particles reduced from 1.41 for the reference sample, to 1.29 for the 0.04 wt% La composite, as shown in Fig. 4. Moreover, the roundness of the particle show an increase trend at La addition beyond 0.04 wt %.

Another interesting effect has caught attention is that the distribution of TiB_2 particles has also been improved, from a severe aggregation to relative dispersion via La addition (Fig. 2). But just like the size and roundness, the distribution of TiB_2 particles also deteriorates when extra La was added into the composite.

3.1.3. TEM analysis

From Fig. 5, acquiring from Cu-1TiB_2-0.08La, (a) presents the TEM observation of TiB_2 morphology. In Fig. 5 (b), it can be seen a lot of twins in the copper matrix, and the twins bend due to the prevention of particles in deformation. The interaction between TiB_2 particles and dislocations is also observed in the TEM image in Fig. 5 (b), it can be clearly seen that the dislocations pile up around TiB_2 particles after the deformation. Furthermore, the interface between copper and TiB_2 was perceptible from HRTEM images. The interface bonding state between copper and TiB_2 is shown in Fig. 5 (c) and (d), which indicates that in situ synthesized TiB_2/Cu composites own well interface and can result in a better mechanical properties.

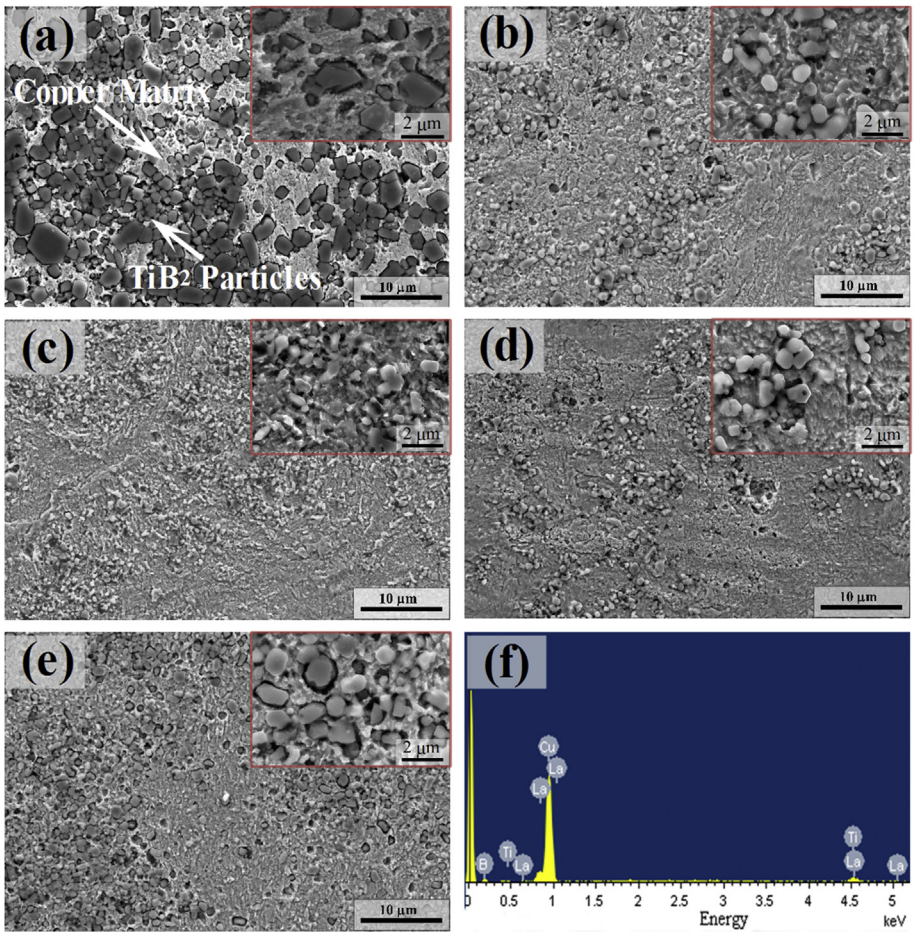

Fig. 2. SEM micrographs of Cu-1 wt% TiB_2 composite with different amount of La addition: (a) without La, (b) 0.02 wt% La, (c) 0.04 wt% La, (d) 0.06 wt% La, (e) 0.08 wt% La, (f) EDS of the 0.04 wt% La composite.

3.1.4. Effect of La on the TiB_2 size and nucleation

The present results in Figs. 2–4 show the significant effects of La on the TiB_2 reinforcing particles in copper matrix. The size of TiB_2 particle decreases and the shape of TiB_2 changes from irregular angular shape to nearly roundness with the increase of La contents. It can be attributed to the unique properties of rare earth La element.

TiB_2 particles are generated from free Ti and B atoms in copper melt, and critical free energy is necessary for the transformation from initial TiB_2 clusters into stable TiB_2 particles. The total energy of the embryo TiB_2 particle is composed of the bulk free energy and interfacial free energy terms. From ref. [32], if the energy of the interface is isotropic and no elastic strain energy is present, the equation could be written as:

$$\Delta G_p = \Delta G_{bulk} + \Delta G_{interfacial} = N\left(\mu_\beta - \mu_\alpha\right) + N^{2/3}\sum_i \gamma_i \eta_i \qquad (1)$$

where ΔG_p, ΔG_{bulk} are the generated free energy and the bulk free energy of TiB_2 particle, $\Delta G_{interfacial}$ is the interfacial free energy of the melt and TiB_2 particle, respectively, μ_α and μ_β are the chemical potentials of the matrix and TiB_2, η_i is a shape factor of ith unit, and γ_i is the interfacial energy of the ith unit interfacial area.

According to ref. [26,32], the interfacial energy term is positive and the bulk free energy is negative. With the increasing number of the cluster molecules N, the free energy ΔG_p has a maximum. This means that there is a barrier to the formation of large stable TiB_2 particle. For this reason, the critical number of molecules Nc and critical free energy of nucleation ΔG_{pc} could be defined. Therefore, the equation is given by:

$$N_c = -\frac{8}{27}\left(\frac{\sum_i \gamma_i \eta_i}{\mu_\beta - \mu_\alpha}\right)^3 \qquad (2)$$

According to equations (1) and (2),

$$\Delta G_{pc} = \frac{4}{27}\frac{\left(\sum_i \gamma_i \eta_i\right)^3}{\left(\mu_\beta - \mu_\alpha\right)^2} \qquad (3)$$

As we known, La element, one of the representative rare earth elements, is a typical surface-active materials, and it has considerably lower surface tension than that of molten Cu, thereby decreasing the surface tension of the melt significantly [33]. And ΔG_{pc} varies as γ^3 in equation (3), which means the critical free energy of nucleation is sensitive to the interfacial energy. So the decreasing of surface energy γ^3 leads to a lower critical free energy. Therefore, the size of TiB_2 critical nucleus decreases a lot, resulting in an increasing probability of nucleation. So, the same amount of Ti and B atoms but more nuclei give a smaller TiB_2 particle size in the composite.

It is known that the wettability of a solid surface by a liquid is

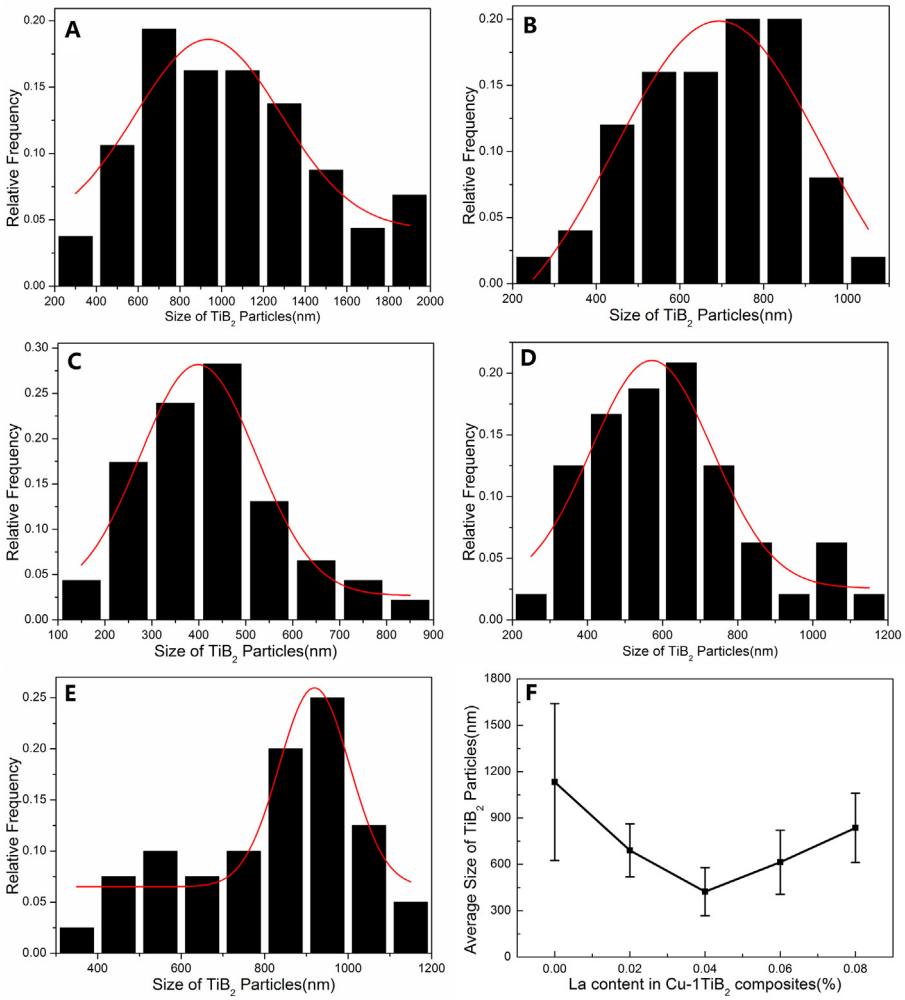

Fig. 3. The size distribution of TiB_2 particles in copper matrix with different amount of La addition: (a)–(e) 0, 0.02, 0.04, 0.06, 0.08; (f) the average size of TiB_2 particles as a function of the La content.

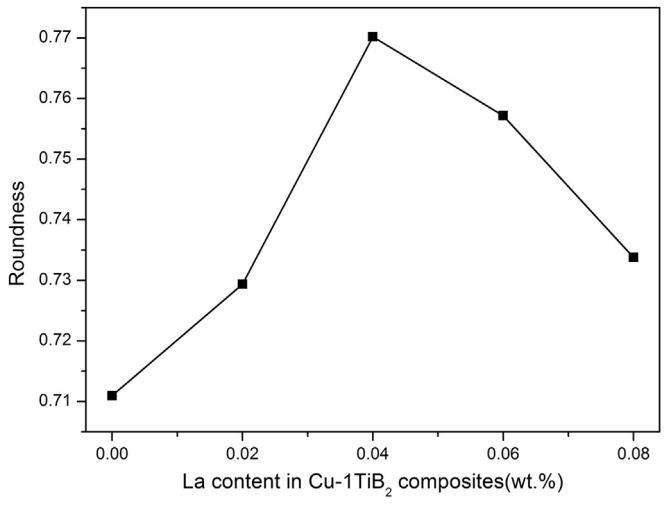

Fig. 4. Roundness of TiB_2 particles as a function of the La content.

quantified by contact angle, which is controlled by the surface tension of the solid-liquid (γ_{sl}), solid-gas (γ_{sg}) and liquid-gas (γ_{lg}). The contact angle θ is determined from these quantities by Young's equation [34,35]:

$$cos\theta = \frac{\gamma_{sg} - \gamma_{sl}}{\gamma_{lg}} \quad (4)$$

As mentioned before, the addition of rare earth La induces a decrease in the surface tension of solid-liquid interface (γ_{sl}), resulting in a lower contact angle, then a better wettability between the liquid and initial particle is acquired. Therefore, the sufficient wetting between the liquid and the TiB_2 particles leads to an obvious smoothening of the initial irregularly shaped TiB_2 particles. And more round reinforced particles are obtained.

The EDS analysis of Cu-1TiB_2-0.08La is shown in Fig. 6, in which Ti, B and La elements exhibit similar distribution. That is to say, La has an important effect on the generating of TiB_2 particles, which has also confirmed the above theory.

Moreover, there are temperature fluctuations in the composites melt, and surface tension is a function of temperature, therefore the fluid flow occurs from a region of low surface tension to a region of high surface tension, that is, the surface tension temperature coefficient is negative [36]. The literature indicates that the addition of La element increases the surface tension temperature coefficient, driving an increasement of the magnitude of the thermocapillary force [26]. Therefore, the capillary forces exerted on the solid TiB_2 particles by wetting matrix liquid are improved. This results in the

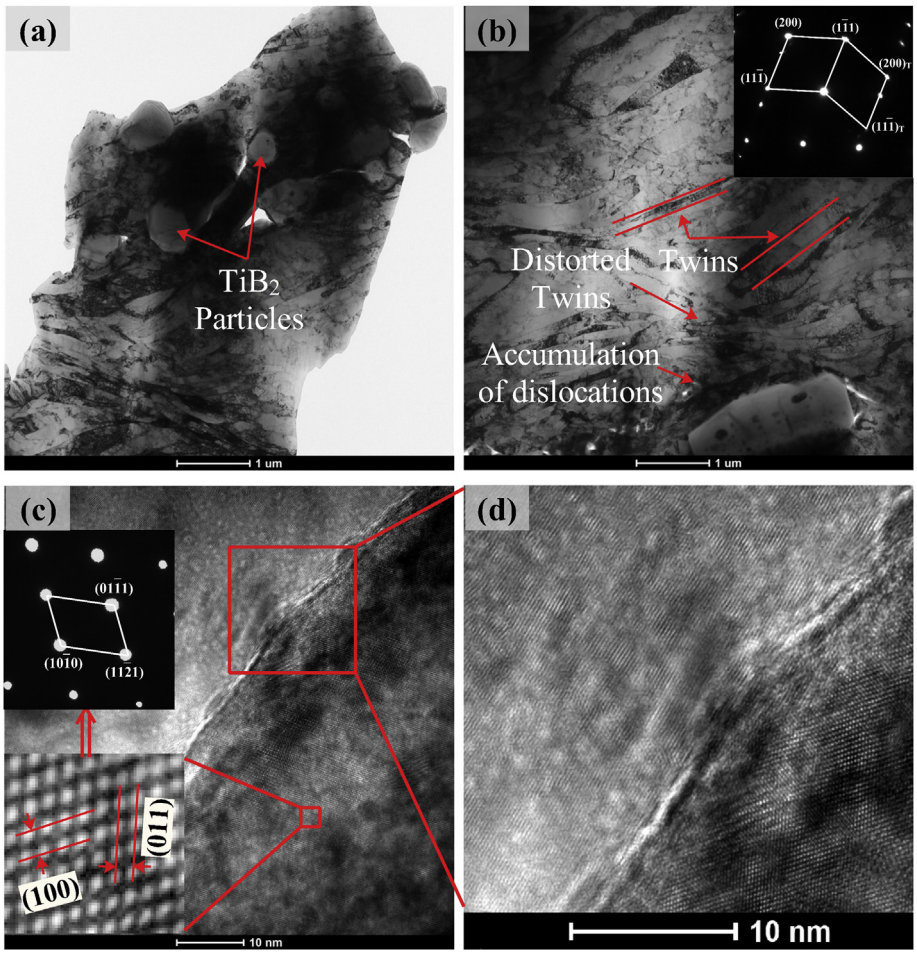

Fig. 5. TEM images of Cu-TiB-La composite (a) TiB_2 particles in copper matrix (b) Twins and dislocations interact with TiB_2 particles (c) Interface between copper and TiB_2 (d) High magnification of (c).

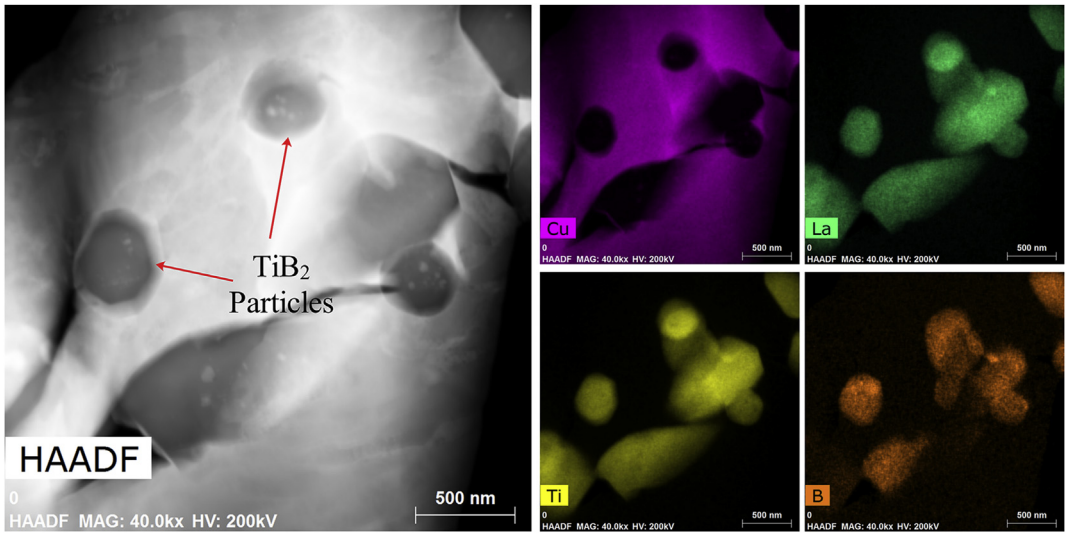

Fig. 6. EDS analysis of Cu-1TiB_2-0.08La.

flow of the melt, then up-grading the penetration rate of the liquid into the voids between the reinforcing particles. Therefore, with the addition of La, better distribution of TiB_2 particles in the matrix was obtained. However, the enhancing liquid flow also gives rise to a higher risk of collision among the TiB_2 particles, so there a tradeoff between the improvement and the amount of La.

3.2. Mechanical properties

The mechanical properties of the Cu-1TiB_2 with different La contents are shown in Table 1. In general, the mechanical properties of the composites versus La addition contents exhibit an inverse relationship with the average particle size as mentioned above. The ultimate tensile strength (UTS) reached its maximum value 507.5 MPa at 0.04 wt% La. However, when the content of La continued rising to 0.06% and 0.08%, the tensile strength slightly decreased to 501 MPa. These variations of tensile properties are mainly attributed to the microstructural change of the TiB_2 particle reinforced CMCs aforementioned. The elongation at maximum stress is shown in the Table 1. It shows a similar tendency with yield strength and more stable than the elongation at break. The elongation at maximum stress increased with the La addition, but decreased when the La over 0.04%. The improvement can be attribute to the size decrease and shape changing of TiB_2 particles. However, more La addition deteriorates the size and morphology of TiB_2 particles and more aggregations appear in the copper matrix. Therefore, the elongations at maximum stress decreased.

The typical stress-strain curves obtained with various La content are presented in Fig. 7. As shown in the figure, the ultimate flow stress for the room temperature sample (Curve of Cu-1TiB_2-0.04La) is approximately 510 MPa. The corresponding yield strength value of this specimen is 479 MPa. As the La contents range from 0 to 0.08%, the flow stress curves exhibit a similar tendency with the variation of strain.

The hardness with error margin of Cu-1TiB_2 composite against different La contents also show in Table 1. The variation of hardness is roughly identical to that of the UTS. Compared to the reference composite, when the La addition level was not too high (in this case, under 0.04 wt%), the hardness of the composite reveals a marked improvement, from about 135 HV to 140 HV in the range from 0.02 to 0.04 wt% La. However, at high addition level, a rapid drop in hardness is evident, to about 132 HV.

The mechanical properties of the composites given in Table 1 and Fig. 7 demonstrate an apparent improvement by La addition. Needless to say, this improvement is mainly ascribed to the particle refinement and dispersion of TiB_2 particles upon La addition.

Several mathematical models have been reported for the yield strength of particle reinforced metal matrix composites (PRMMCs) [13,37,38]. The total yield strength of the PRMMCs is mainly contributed by four mechanisms: grain refinement, Orowan strengthening, coefficients of thermal expansion (CTE) strengthening and load bearing strengthening.

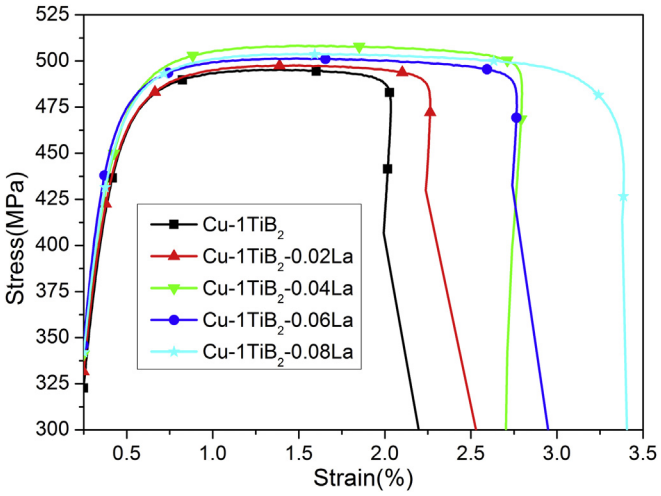

Fig. 7. Stress-strain curves of Cu-1 wt%TiB_2 with different content of La.

In most of the cases, the Orowan mechanism plays a dominant role in strengthening the composites. The shear stress that dislocations need to bypass the particles can be written as [39]: $\tau = Gb/L$, where G and b are shear modulus of the matrix and burgers vector, respectively, and L is the spacing between impenetrable particles. So the smaller the reinforcing particles are, the higher the yield strength of the composite will have. And according to the literature, the Orowan strengthening will show most notably when the particles are smaller than 1 μm. From the histograms in Fig. 3, one can see that nearly half of the TiB_2 particles in the reference composite without La addition are coarser than 1 μm, while after adding 0.04 wt% La, no particles larger than 1 μm can be identified from the entire view of the SEM micrograph. This is why the composite with La addition showed superior mechanical performances with respect to the reference sample.

Moreover, according to the reports in the references [37,40], the total yield strength of the PRMMCs can be written as follow:

$$\sigma_c = \sigma_m + \Delta\sigma_{gf} + \left((\Delta\sigma_{Orowan})^2 + (\Delta\sigma_{CTE})^2\right)^{1/2} + \Delta\sigma_{Load}$$
$$= \sigma_m + \Delta\sigma_{gf} + \left(\left(\frac{0.4MG_m b\ln\left(\sqrt{2/3}d_p/b\right)}{\pi\sqrt{2/3}d_p\left(\sqrt{\pi/4V_p}-1\right)\sqrt{1-\nu}}\right)^2 + \left(\beta G_m b\sqrt{\frac{A\Delta\alpha\Delta T V_p}{bd_p(1-V_p)}}\right)^2\right)^{1/2} + 0.5V_p\sigma_m \quad (5)$$

where σ_c is the yield strength of the composite and σ_m, $\Delta\sigma_{gf}$, $\Delta\sigma_{Orowan}$, $\Delta\sigma_{CTE}$ and are $\Delta\sigma_{Load}$ are the contribution of matrix, grain fine,

Table 1
Mechanical properties of Cu-TiB_2-La composites.

La content in Cu-1TiB_2 (wt%)	σ_b (MPa)	$\sigma_{0.2}$ (MPa)	Hardness (HV)	Elongation at maximum stress (%)
0	495.8	462.6	136.5 ± 6.0	1.25 ± 0.14
0.02	495.2	466.1	134.5 ± 5.6	1.47 ± 0.13
0.04	507.5	478.9	140.7 ± 5.7	1.59 ± 0.05
0.06	501.2	477.3	131.7 ± 5.1	1.50 ± 0.14
0.08	502.8	471.9	131.7 ± 4.2	1.46 ± 0.16

Orowan strengthening, coefficient of thermal expansion strengthening and load bearing strengthening for the yield strength of the composite. And V_p is the volume fraction of reinforced particles; M is the mean orientation factor; G_m is the shear modulus; b is the Burger's vector; d_p is the average particle size; E_m is the Young's modulus of the matrix; ν is the Poisson's ratio and λ is the interparticle spacing; A is a constant of 12; $\Delta\alpha$ is the difference between the CTE of matrix and reinforcement; ΔT is the difference between the processing and test temperatures, respectively. In the prepared composite samples, if the particles aggregate as clusters in the matrix, their contribution to the yield strength will be invalid. These effects can cause the practical mechanical properties severely deviated from the theoretical prediction. Those particles in clusters are called invalid reinforcing particles, which occupy a part of volume fraction of V_p. So, a coefficient, ε has been introduced to relate V_p with the effective TiB_2 fraction V_p^*, to account for the practical strengthening of composites as: $V_p^* = \varepsilon V_p$, where ε is a constant related to the experimental data. Therefore, a severe aggregation will result a lower strength. So, with higher La addition levels, the composites which have more severe aggregation of TiB_2 particles show a degradation in the strength.

3.3. Electrical conductivity

It is interesting to note the change in electrical conductivity of the Cu-1 wt%TiB_2 composites with different La addition. As shown in Fig. 8, it can be seen that the addition of La results in a significant increase in the conductivity of the Cu-1 wt%TiB_2 composites. A nearly 20%IACS increase (from 70%IACS to about 90%IACS) indicates that the conductivity of the composite benefits from La addition. Unlike the mechanical properties, the conductivity shows relatively less notable sensitivity to the content change in La addition.

In this work, we also observed an evident improvement in the electrical conductivity of the Cu-TiB_2 composite, as shown in Fig. 8. According to Matthiessen's rule [41,42], the total resistivity of a crystalline metallic specimen is the sum of the resistivity due to thermal agitation of the metal ions of the lattice and the resistivity due to imperfections in the crystal. This expression could be written as:

$$\rho = \rho(T) + \rho_i \tag{6}$$

where ρ is the total resistivity of the metal or alloy, $\rho(T)$ is the resistivity of the metal which varies with temperature and ρ_i is the resistivity induced by chemical and physical defects which have no relationship with temperature, i.e. the resistivity of a metal resulting from the scattering of conduction electrons. The impurity atoms, interstitials, dislocations, and grain boundaries scatter conduction electrons because of the electrostatic potential difference between their immediate vicinity and that of the perfect crystal structure. Furthermore, it is well known that the solute atoms also have a detrimental influence on resistivity [43]. The impurities in the Cu-TiB_2 composites, such as oxygen, sulphur, and so on, may impair the conductivity significantly. It has been reported that La can preferentially react with these impurities, forming refractory binary or polybasic compounds, and precipitates into or floats off the melt [27,44]. This purifying effect reduces the level of solution atoms in the composites, elevating the conducting efficiency of the material. In addition, the improved distribution instead of aggregation of TiB_2 particles, also decrease the scattering level. This also offered some attribution to the increase in conductivity. Higher La addition levels, however, lead to a slight decrease in conductivity because the re-aggregation of TiB_2 particles in the copper matrix, as shown in Fig. 2d and e.

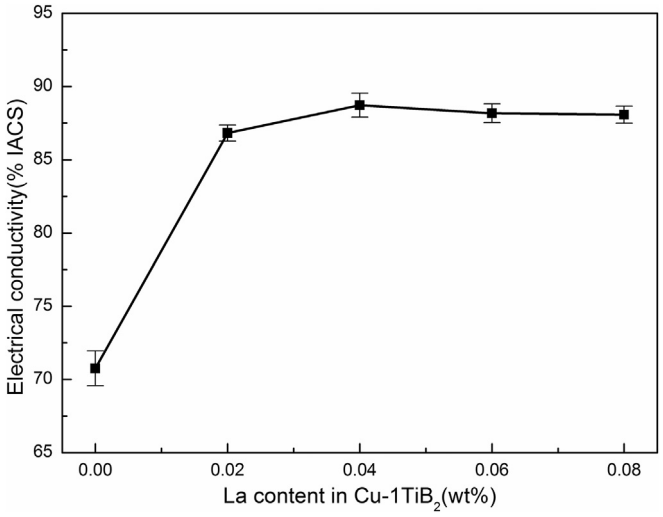

Fig. 8. Electrical conductivity of the Cu-1 wt% TiB_2 composite as a function of the La content.

4. Conclusions

TiB_2 reinforced CMCs were synthesized by in-situ reaction between Cu-B and Cu-Ti. A detailed investigation of the effects of trace La addition on the microstructure and properties of Cu-TiB_2 composites was performed. The following conclusions are drawn based on the results of this work.

(1) The optimum content of 0.04 wt% La significantly decreases the average size of TiB_2 particles, which is 425 nm for the 0.04 wt% La composite, recording a 68% reduction in the average particle size. Besides, the TiB_2 particles are distributed more uniformly due to the trace La addition. These two effects are mainly attributed to the reduced surface tension of the melt by introducing La, as a surface-active agent.
(2) Benefiting from the refined size and improved distribution of TiB_2 particles in the copper matrix, the La added Cu-TiB_2 composite, when follows an appropriate range of La addition, will exhibit superior mechanical performances.
(3) The purifying effect of rare earth La helps to remove the unwanted solution atoms, and makes a considerable increase in the electrical conductivity of the composite as a result.

Acknowledgements

The authors gratefully acknowledge the supports of National Natural Science Foundation of China (Nos. 51525401, 51274054, U1332115, 51401044), the China Postdoctoral Science Foundation (2015M581331), and the Fundamental Research Funds for the Central Universities.

References

[1] K. Lu, The future of metals, Science 328 (2010) 319–320.
[2] Tan Yuehua, Yan Bo, Gao Ge, Yang Yuxin, Effects of substrate local strain on microstructure of electrodeposited aluminum film, J. Wuhan Univ. Technol. Mater. Sci. Ed. 21 (2006) 69.
[3] Chapter V E.S. Machlin, Heterophase and homophase fluctuations, in: E.S. Machlin (Ed.), An Introduction to Aspects of Thermodynamics and Kinetics Relevant to Materials Science, third ed., Elsevier Science Ltd, Oxford, 2007, pp. 159–183.
[4] W. Zhai, W.L. Wang, D.L. Geng, B. Wei, A DSC analysis of thermodynamic properties and solidification characteristics for binary Cu–Sn alloys, Acta Mater. 60 (2012) 6518–6527.
[5] C. Biselli, D.G. Morris, N. Randall, Mechanical alloying of high-strength copper-alloys containing TiB_2 and Al_2O_3 dispersoid particles, Scr. Metall. Mater. 30

(1994) 1327–1332.
[6] M.A. Korchagin, D.V. Dudina, Application of self-propagating high-temperature synthesis and mechanical activation for obtaining nanocomposites, Combust. Explos. Shock Waves 43 (2007) 176–187.
[7] M. Guo, K. Shen, M. Wang, Relationship between microstructure, properties and reaction conditions for Cu-TiB2 alloys prepared by in situ reaction, Acta Mater. 57 (2009) 4568–4579.
[8] A.K. Lee, L.E. Sanchezcaldera, S.T. Oktay, N.P. Suh, Liquid-metal mixing process tailors mmc microstructures, Adv. Mater. Process. 142 (1992) 31–34.
[9] J.H. Kim, J.H. Yun, Y.H. Park, K.M. Cho, I.D. Choi, I.M. Park, Manufacturing of Cu-TiB2 composites by turbulent in situ mixing process, Mater Sci. Eng. A Struct. Mater. Prop. Microstruct. Process 449 (2007) 1018–1021.
[10] M. Sobhani, A. Mirhabibi, H. Arabi, R.M.D. Brydson, Effects of in situ formation of TiB2 particles on age hardening behavior of Cu-1 wt% Ti-1 wt% TiB2, Mater Sci. Eng. A Struct. Mater. Prop. Microstruct. Process 577 (2013) 16–22.
[11] J. Zhang, S. Liu, Y. Zhang, Y. Dong, Y. Lu, T. Li, Fabrication of woven carbon fibers reinforced Al-Mg (95-5 wt%) matrix composites by an electromagnetic casting process, J. Mater. Process. Technol. 226 (2015) 78–84.
[12] S.C. Tjong, Z.Y. Ma, Microstructural and mechanical characteristics of in situ metal matrix composites, Mater. Sci. Eng. R Rep. 29 (2000) 49–113.
[13] T. Wang, Z. Chen, Y. Zheng, Y. Zhao, H. Kang, L. Gao, Development of TiB_2 reinforced aluminum foundry alloy based in situ composites–Part II: enhancing the practical aluminum foundry alloys using the improved Al–5 wt %TiB_2 master composite upon dilution, Mater. Sci. Eng. A 605 (2014) 22–32.
[14] I.A. Ibrahim, F.A. Mohamed, E.J. Lavernia, Particulate reinforced metal matrix composites — a review, J. Mater. Sci. 26 (1991) 1137–1156.
[15] Z. Chen, T. Wang, Y. Zheng, Y. Zhao, H. Kang, L. Gao, Development of TiB_2 reinforced aluminum foundry alloy based in situ composites–Part I: an improved halide salt route to fabricate Al–5 wt%TiB_2 master composite, Mater. Sci. Eng. A 605 (2014) 301–309.
[16] C.-C. Zhu, Y. Li, X.-D. He, X.-H. Zhang, J.-C. Han, Study on the behavior in thermal shock and ablation resistance of TiC-TiB 2/Cu ceramic-matrix composite, J. Aeronaut. Mater. 23 (2003) 15–19.
[17] G.A. Bagheri, The effect of reinforcement percentages on properties of copper matrix composites reinforced with TiC particles, J. Alloys Compd. 676 (2016) 120–126.
[18] T. Tayeh, J. Douin, S. Jouannigot, M. Zakhour, M. Nakhl, J.-F. Silvain, et al., Hardness and Young's modulus behavior of Al composites reinforced by nanometric TiB_2 elaborated by mechanosynthesis, Mater. Sci. Eng. A 591 (2014) 1–8.
[19] J. Ružić, J. Stašić, V. Rajković, D. Božić, Synthesis, microstructure and mechanical properties of ZrB_2 nano and microparticle reinforced copper matrix composite by in situ processings, Mater. Des. 62 (2014) 409–415.
[20] J.P. Tu, N.Y. Wang, Y.Z. Yang, W.X. Qi, F. Liu, X.B. Zhang, et al., Preparation and properties of TiB2 nanoparticle reinforced copper matrix composites by in situ processing, Mater. Lett. 52 (2002) 448–452.
[21] D.Y. Ying, D.L. Zhang, Processing of Cu-Al2O3 metal matrix nanocomposite materials by using high energy ball milling, Mater Sci. Eng. A Struct. Mater. Prop. Microstruct. Process 286 (2000) 152–156.
[22] Basu SN, Hubbard KM, Hirvonen JP, Mitchell TE, Nastasi M. Microstructure and stability of TiB_2 and Cu multilayers1990.
[23] S. Dallaire, J.G. Legoux, Synthesis of TiB_2 in liquid copper, Mater. Sci. Eng. A Struct. Mater. Prop. Microstruct. Process 183 (1994) 139–144.
[24] M.X. Guo, M.P. Wang, K. Shen, L.F. Cao, Z. Li, Z. Zhang, Synthesis of nano TiB2 particles in copper matrix by in situ reaction of double-beam melts, J. Alloys Compd. 460 (2008) 585–589.
[25] Y. Chen, M. Cheng, H.W. Song, S.H. Zhang, J.S. Liu, Y. Zhu, Effects of lanthanum addition on microstructure and mechanical properties of as-cast pure copper, J. Rare Earths 32 (2014) 1056–1063.
[26] D. Gu, Y. Shen, L. Zhao, J. Xiao, P. Wu, Y. Zhu, Effect of rare earth oxide addition on microstructures of ultra-fine WC–Co particulate reinforced Cu matrix composites prepared by direct laser sintering, Mater. Sci. Eng. A 445–446 (2007) 316–322.
[27] F.A. Guo, C.J. Xiang, C.X. Yang, X.M. Cao, S.G. Mu, Y.Q. Tang, Study of rare earth elements on the physical and mechanical properties of a Cu–Fe–P–Cr alloy, Mater. Sci. Eng. B 147 (2008) 1–6.
[28] H. Zhuo, J.C. Tang, N. Ye, A novel approach for strengthening Cu-Y2O3 composites by in situ reaction at liquidus temperature, Mater Sci. Eng. A Struct. Mater. Prop. Microstruct. Process 584 (2013) 1–6.
[29] L. Deng, B. Zhou, H. Yang, X. Jiang, B. Jiang, X. Zhang, Roles of minor rare-earth elements addition in formation and properties of Cu–Zr–Al bulk metallic glasses, J. Alloys Compd. 632 (2015) 429–434.
[30] T.M. Wang, M.Y. Li, H.J. Kang, W. Wang, C.L. Zou, Z.N. Chen, Effects of trace La additions on the microstructures and properties of nanoprecipitates strengthened Cu-Zr alloys, J. Mater. Res. 30 (2015) 248–256.
[31] A. Křupka, K. Říha, Minimal prerequisites for measuring two-dimensional contour roundness in a particle classification context, Powder Technol. 284 (2015) 486–495.
[32] W. Robert, Balluffi, M. Samuel, W. Allen, Craig Carter, Kinetics of Materials, John Wiley & Sons, New Jersey, 2005.
[33] A.I.S.E. Lilley, Morphology of divalent cation precipitates in alkali halide single crystals, Phys. Status Solidi (A) 32 (1975) 533–539.
[34] T. Young, An essay on the cohesion of fluids, Philosophical Trans. R. Soc. Lond. 95 (1805) 65–87.
[35] T.S. Chow, Wetting of rough surfaces, J. Phys. Condens. Matter 10 (1998) L445.
[36] H.J. Niu, I.T.H. Chang, Selective laser sintering of gas and water atomized high speed steel powders, Scr. Mater. 41 (1999) 25–30.
[37] T. Wang, C. Zou, Z. Chen, M. Li, W. Wang, R. Li, et al., In situ synthesis of TiB2 particulate reinforced copper matrix composite with a rotating magnetic field, Mater. Des. 65 (2015) 280–288.
[38] W.S. Miller, F.J. Humphreys, Strengthening mechanisms in particulate metal matrix composites, Scr. Metall. Mater. 25 (1991) 33–38.
[39] T.W. Clyne, P.J. Withers, An Introduction to Metal Matrix Composites, Cambridge University Press, USA, 1993.
[40] M. Wang, D. Chen, Z. Chen, Y. Wu, F. Wang, N. Ma, et al., Mechanical properties of in-situ TiB_2/A356 composites, Mater. Sci. Eng. A 590 (2014) 246–254.
[41] W.E. Lawrence, J.W. Wilkins, Electron-electron scattering in transport coefficients of simple metals, Phys. Rev. B 7 (1973) 2317–2332.
[42] B. Lengeler, W. Schilling, H. Wenzl, Deviations from Matthiessen's rule and longitudinal magnetoresistance in copper, J. Low. Temp. Phys. 2 (1970) 59–86.
[43] Z. Shijie, Z. Bingjun, Z. Zhen, J. Xin, Application of lanthanum in high strength and high conductivity copper alloys, J. Rare Earths 24 (2006) 385–388.
[44] Z.W. Wu, Y. Chen, L. Meng, Effects of rare earth elements on annealing characteristics of Cu–6 wt% Fe composites, J. Alloys Compd. 477 (2009) 198–204.